Oxidation Rate Effect on the Direction of Metal-Assisted Chemical and Electrochemical Etching of Silicon

Zhipeng Huang,*,†,‡ Tomohiro Shimizu,†,§ Stephan Senz,*,† Zhang Zhang,† Nadine Geyer,† and Ulrich Gösele†

Max Planck Institute of Microstructure Physics, Weinberg 2, D-06120 Halle/Saale, Germany, Functional Molecular Materials Centre, Scientific Research Academy and School of Chemistry and Chemical Engineering, Jiangsu University, Zhenjiang 212013, P. R. China, and Faculty of Engineering Science, Kansai University, 3-3-35 Yamate-cho, Suita-city, Osaka 564-8680, Japan

Received: November 23, 2009; Revised Manuscript Received: April 9, 2010

Assisted by noble metal particles, non-(100) Si substrates were etched in solutions with different oxidant concentrations at different temperatures. The etching directions of (110) and (111) Si substrates are found to be influenced by the concentration of oxidant in etching solutions. In solutions with low oxidant concentration, the etching proceeds along the crystallographically preferred ⟨100⟩ directions, whereas the etching occurs along the vertical direction relative to the surface of the substrate in solutions with high oxidant concentration. These phenomena are found for both *n*- and *p*-type substrates as well as in experiments with different oxidants. The experiments on metal-assisted chemical etching are complemented by additional experiments on metal-assisted electrochemical etching of (111) Si substrates with different current densities. As a function of current density, a change of etching directions is observed. This shows that the change of the etching directions is mainly driven by the oxidation rate. On the basis of these phenomena, we have demonstrated fabrication of Si nanopores with modulated orientations by periodically etching a (111) substrate in solutions of low and high oxidant concentrations.

Introduction

Nanostructures of silicon (Si), which is the most important material in semiconductor industry, have attracted increasing attention over the past decade. Applications of Si nanostructures are not limited to field-effect transistors[1,2] but include solar cells[3–5] and renewable energy devices[6] as well as sensors.[7,8] As in the case of other nanomaterials or nanostructures, the properties of Si nanostructures are determined by their sizes,[9] morphologies,[10] crystallographic orientations,[11,12] and alignment directions relative to the substrate used.[5] Therefore, controllable fabrication is essential for most applications of Si nanostructures.

Among many fabrication methods, metal-assisted chemical etching has gained importance as a low-cost and versatile method for fabricating Si and SiGe nanostructures,[13–16] enabling easy control of position, diameter, and length[17,18] and partially also of the orientation direction of the Si and SiGe nanostructures.[5,14,19–23] In metal-assisted chemical etching, noble metal particles or films with pores are used to catalyze the etching of a Si substrate in a HF solution containing an oxidant. The Si substrate below the noble metal particles or the film is etched much faster than the Si substrate without noble metal coverage. Consequently, by control of the morphology of the deposited noble metal, the resulting morphology of Si nanostructures can be controlled. Various Si nanostructures such as nanowires,[17,18] nanofins,[24] and nanopores[25] have been successfully fabricated with controllable diameters and lengths.

* To whom correspondence should be addressed. E-mail: zphuang@ujs.edu.cn (Z.H.), senz@mpi-halle.mpg.de (S.S.). Fax: +86-511-8879-7815 (Z.H.), +49-345-5511-223 (S.S.).

† Max Planck Institute of Microstructure Physics.

‡ Jiangsu University.

§ Kansai University.

However, a simple approach to control the direction of Si nanostructures fabricated by metal-assisted chemical etching is yet to be developed because metal-assisted chemical etching is influenced by the crystallographic orientation of the Si substrate, similar to what happens in the electrochemical etching of Si[26] (e.g., etching prefers to proceed along ⟨100⟩ directions in metal-assisted chemical etching, even if (110), (111), or (113) substrates are used[19–21]). The etching behavior of (111) substrates remains confusing because in literature preferred etching directions along ⟨100⟩ or [111] have been published.[5,14,20,21] A systematic study of the etching behavior of (111) substrates has not been performed so far.

In this article, we demonstrate that the concentration of the oxidant is an important factor affecting the etching direction of non-(100) substrates (i.e., (111) and (110) substrates). We will first present the etching directions of the (111) substrate in solutions with different oxidant concentrations, which will help us to explain the confusing and partially contradictory results in literature and then show the influence of the oxidant concentration on the etching direction of (110) substrate, which has not been reported in the literature so far. In etching solutions with low oxidant concentrations, the usual crystallographically preferred ⟨100⟩ etching directions prevail, and the etching proceeds in inclined directions with respect to the surface normal, whereas the etching mostly occurs along the surface normal if the concentration of oxidant is sufficiently high. Instead of changing the chemical oxidant concentration to influence the etching direction, the electrochemical etching allows a direct control of the dissolution speed of Si by changing the current density. On the basis of these findings, we can control the etching directions during the etching and are able to fabricate orientation-modulated Si pores.

10.1021/jp911121q
Published on Web 05/27/2010

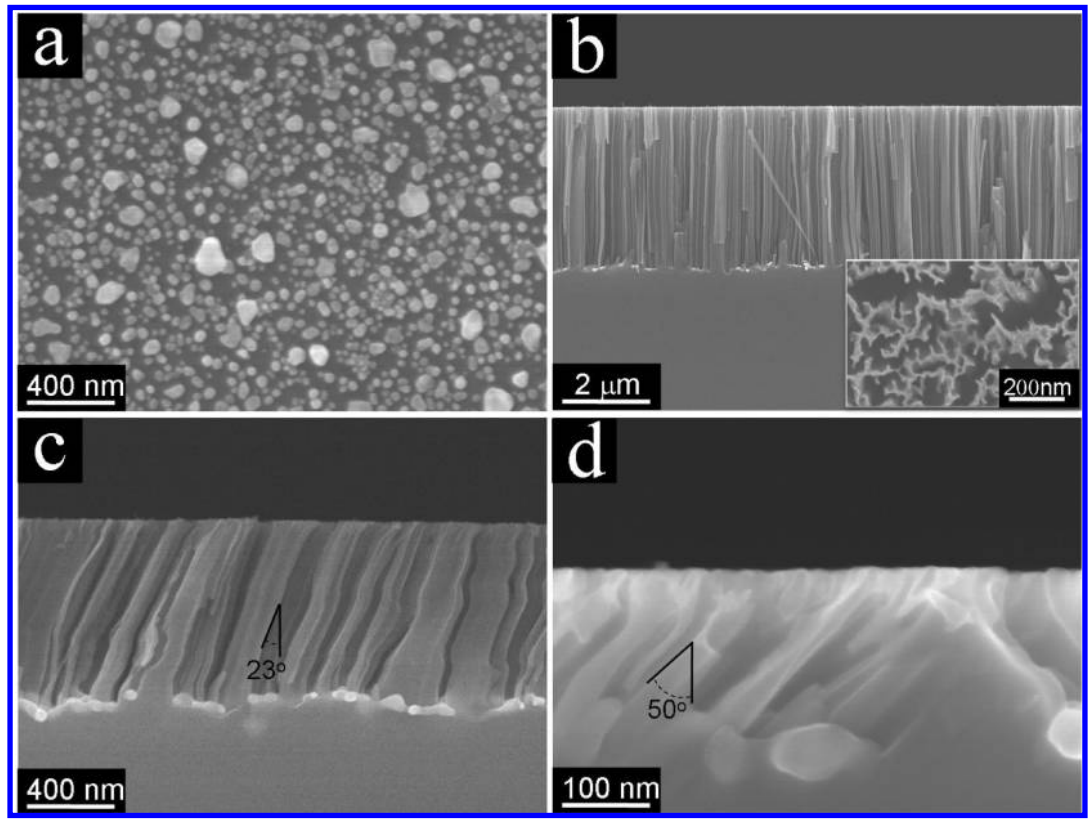

Figure 1. Plan view SEM image of (a) silver particles loaded *p*-type (111) substrate and cross-sectional view SEM images of samples etched in (b) solution I (high $[H_2O_2]$), (c) solution II (medium $[H_2O_2]$), and (d) solution III (low $[H_2O_2]$). Plan view SEM image of sample etched in solution I (inset of b).

Experimental Methods

The Si substrates used this study, which were *p*-type (111) Si (ρ: 1−10 Ω·cm), *n*-type (111) Si (ρ: 1−10 Ω·cm), and *p*-type (110) Si (ρ: 1−10 Ω·cm), were obtained from Silicon Materials (Landsberg am Lech, Germany). Prior to etching, the substrates were cut into 5 × 5 mm^2 pieces. The Si pieces were cleaned by an RCA cleaning procedure ($NH_3 \cdot H_2O/H_2O_2/H_2O$ 1/1/5 v/v/v, 80 °C, 1 h) and then rinsed with copious amounts of deionized water.

Silver was used to catalyze etching in our experiments. The silver particles were deposited onto the Si substrates by electroless plating. The plating solution was a mixture of aqueous solution of silver nitrate and hydrofluoric acid ($[AgNO_3]$ = 2 mM, [HF] = 4.6 mM). The cleaned Si substrates were immersed in the plating solution for 30 s at room temperature with room light illumination. The silver-loaded substrates were rinsed by deionized water and then etched with etching solutions with different concentrations of H_2O_2 in the dark. After the etching, the substrates were rinsed by deionized water and dried on a 100 °C hot plate under an ambient atmosphere.

Six chemical etching solutions were used in our experiments, which were solution I ($[H_2O_2]$ = 100 mM, [HF] = 4.6 M), solution II ($[H_2O_2]$ = 20 mM, [HF] = 4.6 M), and solution III ($[H_2O_2]$ = 2 mM, [HF] = 4.6 M) for the etching of the (111) substrates and solution A ($[H_2O_2]$ = 400 mM, [HF] = 4.6 M), solution B ($[H_2O_2]$ = 1 M, [HF] = 4.6 M), and solution C ($[H_2O_2]$ = 2 M, [HF] = 4.6 M) for the (110) substrates. The etching experiments were conducted at different temperatures, which were 4 °C in a refrigerator, room temperature (ca. 20 °C) under an ambient atmosphere, and 30 and 45 °C in water baths. Before etching, the etching solutions were stored under the desired conditions for >6 h to stabilize the temperature of the solutions.

The electrochemical etching was performed in a Teflon cell at room temperature. A solution of 3.6 wt % HF in water was used. The electrical current was regulated by the power supply to obtain galvanostatic conditions. The plating recipe for the Ag particles was the same as that for the chemical etching.

Scanning electron microscope (SEM, JSM-6701F, JEOL) and transmission electron microscope (TEM, JEM4010F, JEOL) were employed to investigate the morphologies of samples. For cross-sectional view SEM images, samples were cleaved along ⟨112⟩ edges, exposing {111} surfaces. Cross-sectional TEM samples were fabricated by focused ion beam (FIB, Nova Lab 600, FEI) mining. In the FIB mining, the samples were cut parallel to the cleaved edge. A layer of SiO_2 was deposited to fill the pores or the interstice between Si nanowires; then, a Pt layer with thickness of 2 μm was deposited to protect the sample during the mining.

Results and Discussion

Silver deposited on (111) silicon substrates via electroless plating resulted in isolated silver particles on the substrate (Figure 1a); then, the silver-loaded substrates were etched in mixed solutions of HF and H_2O_2. The etching proceeded along different directions depending on the concentrations of H_2O_2 in the etching solutions. The etching showed three typical behaviors, as presented in Figure 1b−d. Cross-sectional view and plan view SEM images of a sample etched in a solution with high H_2O_2 concentration (solution I, $[H_2O_2]$ = 100 mM) (Figure 1b) suggest that etching occurred along the vertical direction of the substrate, which was a [111] direction, leaving behind vertically aligned Si nanopores or nanowires. When the concentration of H_2O_2 was decreased to 20 mM (solution II), the etching began to occur in inclined directions, with the angle relative to the substrate normal ~23°, as shown by the

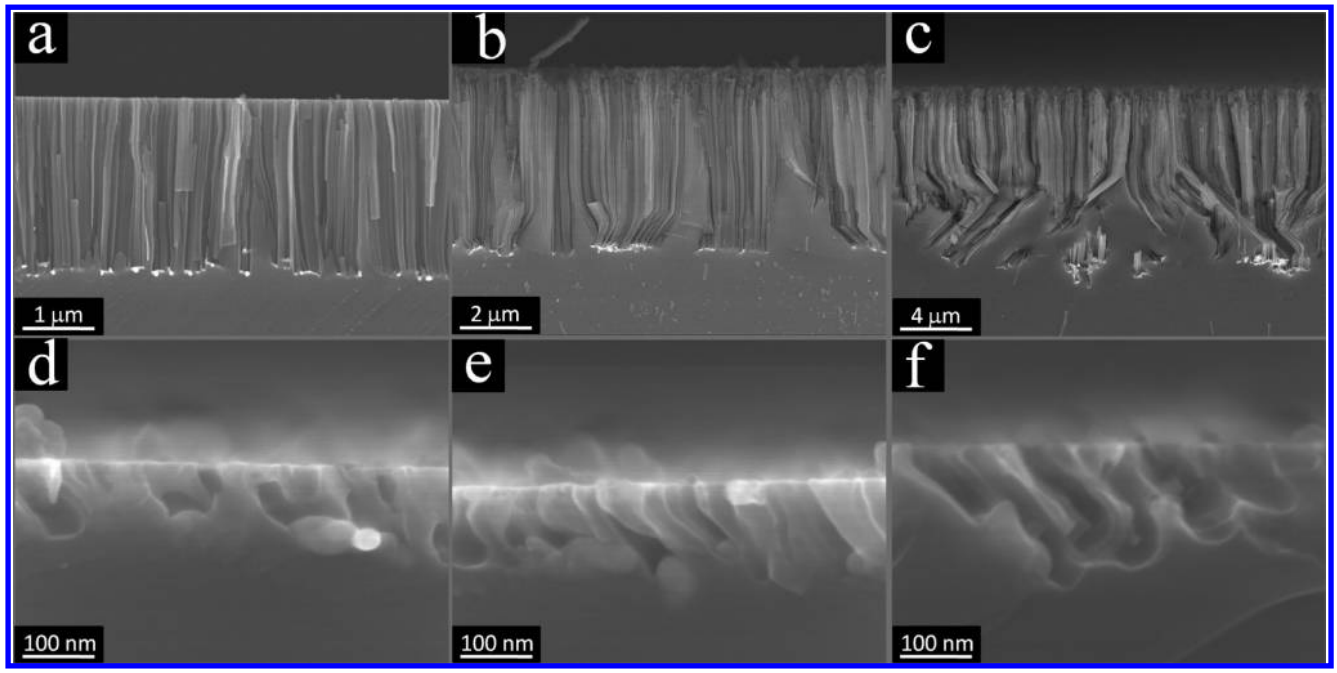

Figure 2. Cross-sectional view SEM images of *p*-type (111) Si substrates etched in solution I for 10 min at (a) 4, (b) 30, and (c) 45 °C and in solution III for 20 min at (d) 4, (e) 30, and (f) 45 °C, respectively.

corresponding cross-sectional view SEM image (Figure 1c). With concentration of H_2O_2 lowered to 2 mM (solution III), the tilt away from the substrate normal increased to ~50° (Figure 1d), suggesting a [100] etching direction.[27] (Also see Figure S1 in the Supporting Information.) This H_2O_2-concentration-related etching occurs not only in *p*-type Si substrates but also in *n*-type substrates (Figure S2 in Supporting Information). For samples etched in solutions with different concentrations of $Fe(NO_3)_3$, which is another frequently used oxidant in metal-assisted chemical etching, the etching directions of (111) substrates also depend on the concentration of $Fe(NO_3)_3$ (Figure S3 in Supporting Information). These observations suggest that the concentration of the oxidant is an important factor affecting etching directions of (111) substrates.

To investigate the origin of different etching directions in different solutions, etching experiments were carried out in different solutions at different temperatures. Figure 2 shows representative results of a series of experiments. Etched with solution III, etching always proceeded in inclined directions, even though the temperature of the etching solutions was varied from 4 to 45 °C. In contrast, etching in solution I varied its directions with temperature. All samples were etched for the same time (10 min) in solution I. At 4 °C and room temperature, the etching occurred along the vertical direction. However, the etching switched its direction from the surface normal to an inclined direction in samples etched at 30 and 45 °C.

Etching rates are different at different temperatures. The higher the temperature is, the faster the etching occurs. After 10 min of etching in solution I, the pores proceed vertically into the substrate for ~2.5 μm at 4 °C (Figure 2a), 3.5 μm at room temperature (Figure 1b), 5 μm at 30 °C (Figure 2b), and 10 μm at 45 °C (Figure 2c), respectively. It is worth noting that the switch of etching direction in samples etched at 30 and 45 °C occurs nearly 4 to 5 μm vertically away from the surface of the substrates, which is larger than the etching depth of samples etched at 4 °C and room temperature. It implies that if the etching at 4 °C and room temperature occurred for longer times, then a switch of etching direction would also occur at these two temperatures.

To verify this assumption, the substrates were etched in solution I at room temperature for 4−24 min. As expected, a switch of etching direction occurred when the etching depth was larger than ca. 4 μm (Figure 3). The cross-sectional SEM images of samples etched for different times show that the etching direction varies gradually from vertical direction to inclined directions and finally maintains one of the ⟨100⟩ directions.

The vertical distances of switch points to the surface of the substrates are similar for samples etched with the same solution at different temperatures, suggesting that the change in etching directions could be ascribed to a solution effect. When etching proceeds to the same depth, the consumption of HF and H_2O_2 should be similar. This solution-dependent etching can be confirmed by etching the substrate in sequence in different solutions. If the concentration of H_2O_2 in the etching solution was reduced by varying the etching solution from solution I to solution III, then the switch of etching direction occurred at a depth of ~200 nm (Figure 4a), which was smaller than the switching depths shown in Figure 3. When etching solution was varied from solution III to solution I, etching switched from inclined ⟨100⟩ directions to the vertical [111] direction (Figure 4b). Accordingly, by periodically varying etching solutions, the etching direction could be periodically switched, resulting in orientation-modulated pores (Figure 4c,d).

Although it has been found that the morphologies of silver particles can affect etching directions[28] and the morphologies of silver particles might change during etching because of slight dissolution of silver in an oxidative solution,[27,29] etching along different directions in solutions with different oxidant concentrations cannot be ascribed to the morphological variations of the silver particles. This assumption can be confirmed by the fabrication of orientation-modulated structures presented in Figure 4c,d. If the morphologies of the silver particles varied and led to a switch of the etching direction from [111] in solution I to [100] in solution III, then the morphologies of the silver particles could not be recovered when etching solutions were changed from solution III to solution I. A switch of the etching direction from [100] to [111] cannot be expected because the

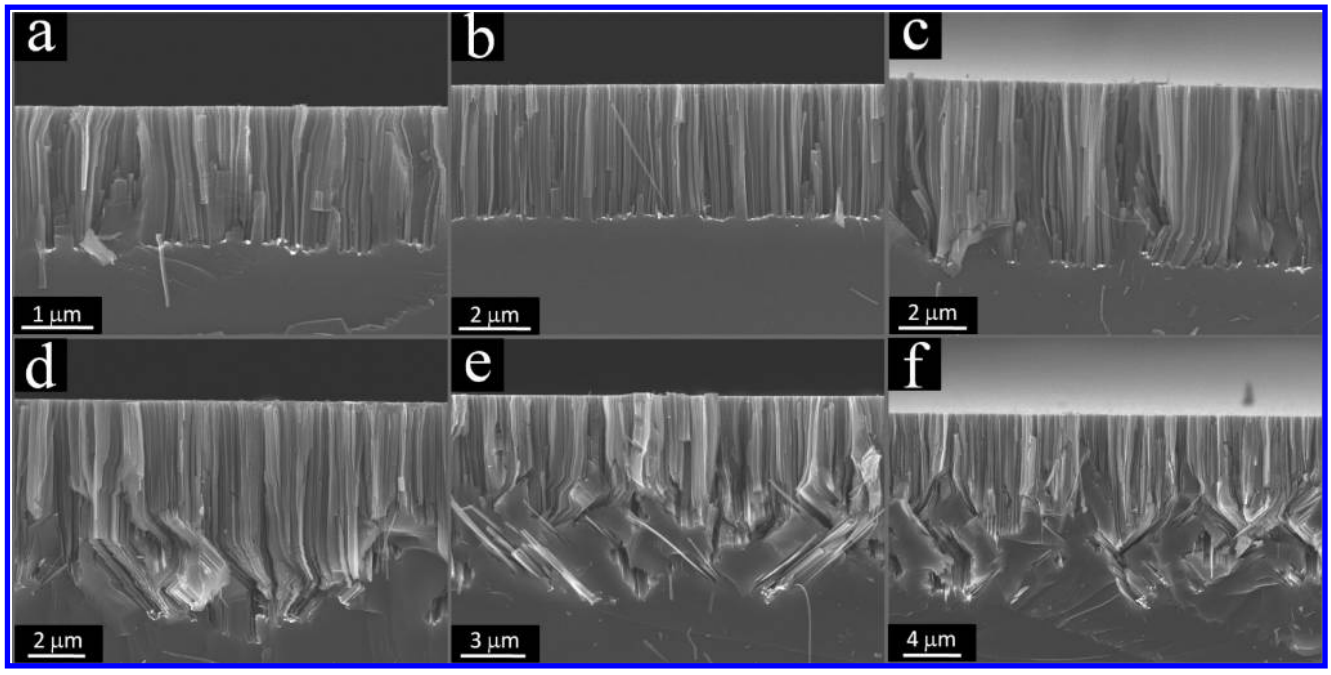

Figure 3. Cross-sectional view SEM images of *p*-type (111) Si substrate etched in solution I at room temperature for (a) 4, (b) 8, (c) 12, (d) 16, (e) 20, and (f) 24 min.

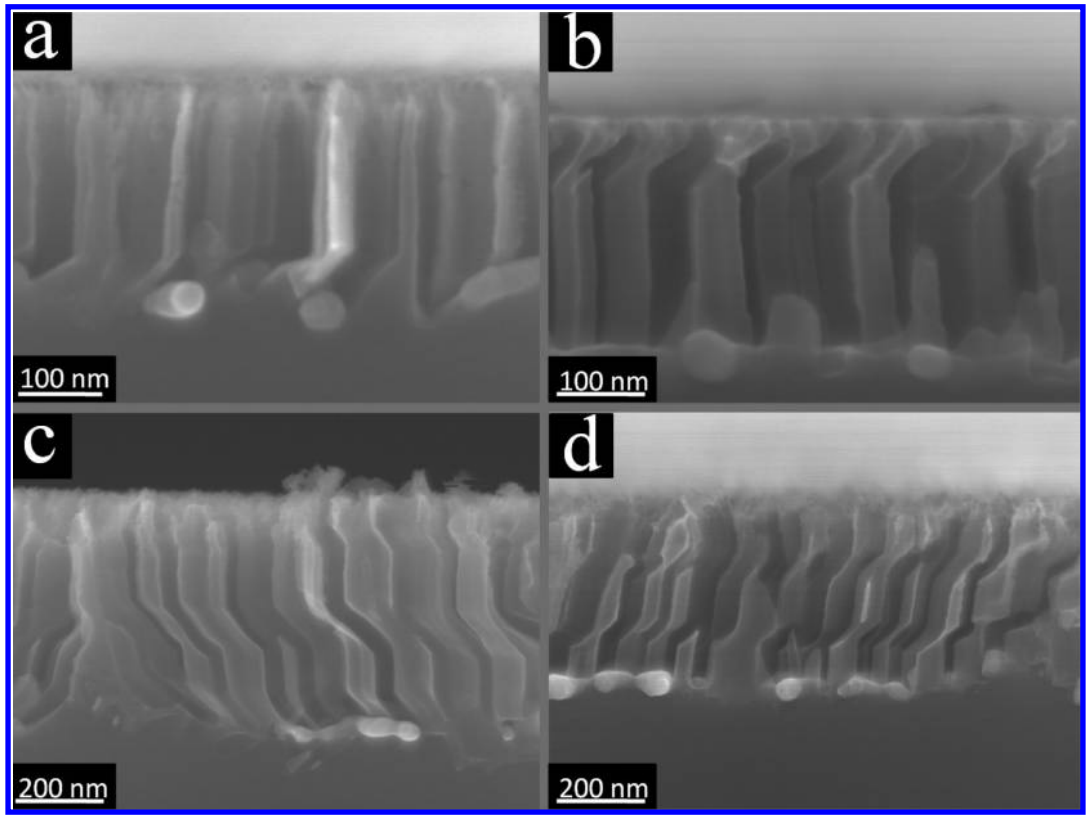

Figure 4. Cross-sectional view SEM images of *p*-type (111) Si substrates etched at 4 °C for (a) 1 min in solution I and then 10 min in solution III and (b) for 10 min in solution III and 1 min in solution I, (c) for three periods of the sequence (1 min in solution I and then 10 min in solution III), and (d) for three periods of the sequence (10 min in solution III and 1 min in solution I).

dissolution of silver in the oxidative solution is an irreversible process, especially because the sample was washed with copious amounts of water after each etching step.

It has been found that the surface morphology of etched structures is affected by the concentration of the etching solution in metal-assisted chemical etching.[25] In solutions with very high HF and H_2O_2 concentrations, walls of etched pores were rough and a layer of porous Si is formed on the walls of the pores.[25] However, the concentrations of HF and H_2O_2 in all solutions we used are much smaller than those reported in ref 25, and no porous layer is found on the walls of the etched structures (Figure 4). To get insight into the morphology of the etching front and the interface between silver particles and Si, we carried out high-resolution TEM (HRTEM) investigations. Figure 5 shows a low-magnification TEM image and a HRTEM image of a pore proceeding along [111] direction. The crystalline Si

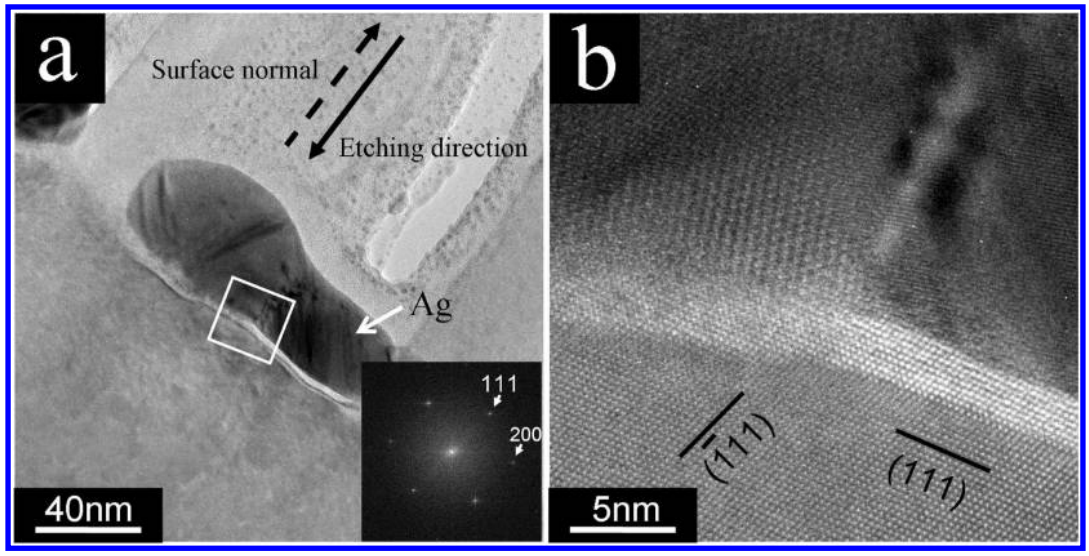

Figure 5. (a) Low-magnification cross-sectional TEM image of *p*-type (111) Si substrate etched along the [111] direction. (a) The solid white arrow indicates a silver particle at the etching front, the solid black arrow indicates the etching direction, and the broken black arrow indicates the direction of the surface normal. Insert shows a fast Fourier transform (FFT) of the TEM image of Si substrate. (b) High-resolution TEM image showing details of Si/Ag interface enclosed by white rectangle in part a. The black lines show the projections of (111) and (1̄11) planes of Si along the direction of electron beam, respectively.

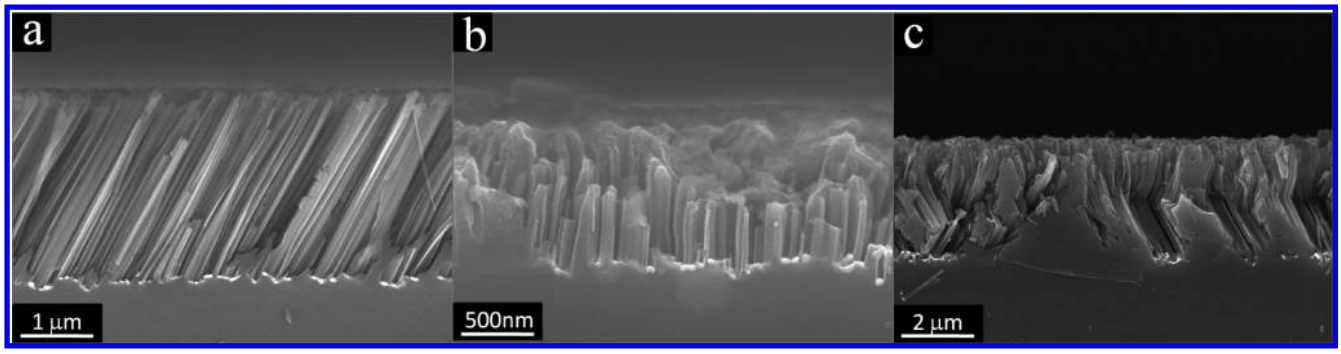

Figure 6. Cross-sectional SEM images of (110) substrates etched at room temperature in (a) solution A for 3 min, (b) solution B for 1 min, and (c) solution C for 3 min.

lattice pattern at the etching front is clearly shown (Figure 5b), in which the bright contrast at the etching front might be attributed to a thinner Si in this region or to the existence of an amorphous oxide in this region. The HRTEM image confirms that the etching front is solid and not porous. Therefore, the interface morphology at the etching front should not be a major factor that induces the vertical [111] etching in our experiments.

Similar phenomena occur in metal-assisted chemical etching of (110) substrates in solution with different oxidant concentrations. In solutions with low H_2O_2 concentrations, the etching proceeds along a [100] direction (Figure 6a, see also ref 22). When the concentration of H_2O_2 is sufficiently high, the etching occurs in the [110] direction, leading to vertically etched structures (Figure 6b). Moreover, a switch of etching direction is also found in the etching of the (110) substrate, provided that the etching time is sufficiently long. Figure 6c shows an example that in the same etching solution the etching occurs first in vertical [110] direction and then proceeds along inclined ⟨100⟩ directions. Therefore, our results imply that the influence of oxidant concentration on the etching direction might be a general phenomenon that happens in non-(100) substrates. Our finding offers an alternative approach to control the etching direction in non-(100) Si substrates via choosing a proper solution, besides control via the lateral size of the metal film used.[22]

The effect of changing etching direction as a function of oxidant concentration is observed for two different oxidants and Si substrates with two different orientations. This leads to the assumption that this observation is a general behavior of the etching of Si. To verify this assumption, we performed the metal-assisted electrochemical etching of Si (111) substrate with different current densities. With low current density, the etching occurs in inclined directions (Figure 7a,b), whereas the etching occurs in the vertical [111] direction with high current density (Figure 7c,d). The results clearly show that the change of the etching direction is mainly influenced by the oxidation rate. Rapid oxidation leads to etching perpendicular to the surface, whereas slow oxidation results in etching along ⟨100⟩ directions.

Independent of the details of the experiments in all three cases, the dissolution of Si requires an electron transfer. The Si in the bulk is electrically neutral, and by removing electrons it can be changed into an ionic state. The positive Si ion cannot be dissolved directly in water. The formation of a negatively charged complex containing fluorine ions or OH^- ions is necessary. In all three cases, the noble metal increases locally the reaction rate. During chemical etching, the walls of the already etched structures are only slowly etched, and a high aspect ratio can be obtained. A similar shape is observed after metal-assisted electrochemical etching. Noble metals (e.g., Ag[30] and Au[31]) are very well-known for their catalytic effect on the

reduction of H_2O_2. In this experiment, the Si atoms need to be removed from the covalent bonds to the Si crystal and change their oxidation state to produce the complex ions. Therefore, in principle, the effect of the metal can be either to break the covalent bonds or to assist the electron transfer.

The change of the etching direction might be understood by a combination of the surface state of Si in different solutions (or current densities) and the back-bond strength,[32] which is used to explain direction dependence of chemical and electrochemical reactions on Si surfaces.[20,33,34] Because of the lattice structure of Si crystals, atoms on {100} planes have two back bonds to the underneath atoms, whereas atoms on {111} planes have three back bonds. Therefore, the atoms on {100} planes are easier to dissolve compared with the atoms on {111} planes, and the substrate is preferentially etched in ⟨100⟩ directions.

The concentration of H_2O_2 and current density affects the surface state of Si in metal-assisted chemical etching and metal-assisted electrochemical etching, respectively. It has been proposed by analogy to the anodic electrochemical etching of Si[35,36] that there are two competing dissolution processes of Si in the metal-assisted chemical etching. The first one is direct dissolution in the divalent state (Model I, as eq 1),[37,38] and the second one is Si oxide formation, followed by the dissolution of oxide (Model II, as eq 2 and 3).[14,20,38–42]

$$Si + 4HF_2^- \rightarrow SiF_6^{2-} + 2HF + H_2 + 2e^- \quad (1)$$

$$Si + 2H_2O \rightarrow SiO_2 + 4H^+ + 4e^- \quad (2)$$

$$SiO_2 + 6HF \rightarrow H_2SiF_6 + 2H_2O \quad (3)$$

If the concentration of H_2O_2 or the current density is low, then the etching is limited by the transfer of electrons, and the dissolution of Si proceeds in a way described by Model I. Consequently, the etching direction of Si should be discussed by considering back-bond strength. As a result, the ⟨100⟩ etching directions prevail in non-(100) substrate. In contrast, Model II prevails if the concentration of H_2O_2 is sufficiently high in metal-assisted chemical etching or current density is sufficiently high in metal-assisted electrochemical etching so that Si oxide is formed at the etching front because the rate of Si oxide dissolved by HF is slower than the formation rate of Si oxide. In this specific case that the etching front is completely covered by the Si oxide, the etching of Si proceeds through the dissolution of the Si oxide layer by HF at the etching front, which is a well-known isotropic process.[26] Both reactions are locally accelerated by the catalytic effect of the noble metal particles. During the etching of Si in HF solution, hole injection from oxidant to Si is essential for the oxidation of Si and either dissolution or formation of Si oxide. The noble metal (e.g., Ag[30] and Au[31]) could catalyze the reduction of H_2O_2, so that the reduction of H_2O_2 is much faster on the surface of the noble metal than on bare Si surface without metal coverage. Accordingly, more holes will be injected into Si through the noble metal/Si interface than through the bare Si surface; therefore, Si oxide prefers to form locally at the noble metal/Si interface. Consequently, oxidation and etching of Si occur preferentially

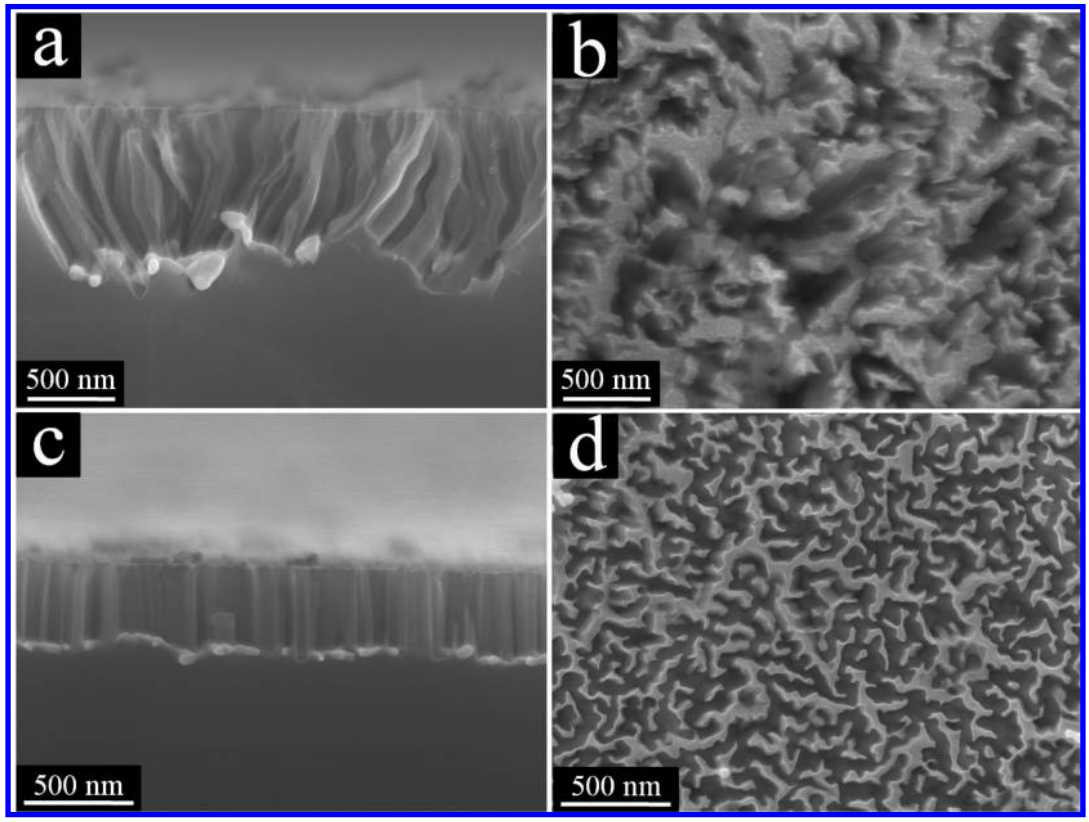

Figure 7. (a) Cross-sectional view and (b) plan view SEM images of Ag-particles-loaded *p*-type Si (111) substrate etched electrochemically with current density $J = 0.2$ mA/cm^2 (etching time: 90 min). (c) Cross-sectional view and (d) plan view SEM images of Ag-particles-loaded *p*-type Si (111) substrate etched electrochemically with current density $J = 4$ mA/cm^2 (etching time: 4 min).

at the noble metal/Si interface, and the etching of Si below noble metal proceeds much faster than the etching of bare Si and the wall of already etched structures. Therefore, even if the dissolution of Si oxide by HF is isotropic, the etching appears more like anisotropic, along the vertical direction, because of the catalytic effect of the noble metal.

Influence of surface state on the back-bond strength is also found in the alkaline solution etching of Si, where surface termination varies from Si−H to Si−OH in the presence of an oxidizing agent, and Si−OH bonds enable weakening of Si back bonds and reduce anisotropy.[43] Therefore, in metal-assisted chemical/electrochemical etching, even if the concentration of H_2O_2 or current density is not high enough to form a continuous Si oxide but remains sufficiently high to form Si−OH surface bonds, the back-bond strength can be weakened, and the etching deviates from the crystallographically preferred ⟨100⟩ directions.

The above-mentioned model implies that if the ratio between HF and H_2O_2 concentrations ([HF]/[H_2O_2]) is sufficiently high so that the dissolution rate of Si oxide is faster than the formation rate of Si oxide, then Si oxide or Si−OH bonds cannot form and the etching will proceed in inclined direction even if the concentration of H_2O_2 is high (e.g., as high as in solution I). This assumption can be confirmed by experiment. The Si (111) substrate has been etched in an etchant in which the concentration of H_2O_2 is as high as that in solution I, whereas the [HF]/[H_2O_2] is as high as that in solution II. The etching direction does deviate from the vertical direction (Figure S4 in Supporting Information), confirming the model we proposed.

Accordingly, the actual etching direction is a result of a competition between ⟨100⟩ etching, determined by back-bond strength, and vertical etching, due to weakening of back-bond strength. If the concentration of oxidant or current density is sufficiently large, then vertical etching prevails (Figures 1b and 7c), whereas crystallographically preferred ⟨100⟩ etchings are pronounced (Figure 1d) if the concentration of the oxidant is sufficiently small. Otherwise, etching proceeds between the vertical direction and the ⟨100⟩ directions (Figure 1c).

In the initial stage of etching, the silver particles tend to move vertically into the Si substrate if the concentration of oxidant is sufficiently large. With the etching proceeding, etched pores extend further and further into the Si substrate. In this case, the oxidant in the pores is consumed, and the concentration of oxidant near the etching front in the etched pores is reduced and has to be supplied by oxidant diffusion from the bulk solution into the pores.[44] With the decrease in oxidant concentration, the surface state of Si might vary. Consequently, the etching switches gradually from the vertical [111] direction, to inclined directions, and finally to ⟨100⟩ directions (Figure 3). Therefore, in experiments, it can be found that the etching proceeds initially in the vertical [111] direction and finally in ⟨100⟩ directions if the etching time is long enough.[20,21]

In this article, we present that the oxidation rate is an important factor affecting the etching direction of non-(100) substrates under otherwise identical conditions. It is worth noting that the etching direction of Si is affected by many factors beside crystallographic orientation of Si substrate and the concentration of the oxidant or the current density. Tsujino et al. found that the shape of the Ag particle can affect the etching direction.[15] That is, Ag with irregular shape resulted in random etching leading to disordered structures, whereas the etching varied from random directions to the vertical [100] direction in a (100) substrate when the shape of Ag particle became round because of the slow dissolution of Ag.[15] We also found that the connection between Ag particles influenced the etching direction.[22] When isolated Ag particles were used, the etching proceeded along crystallographically preferred ⟨100⟩ directions, whereas the etching proceeded along the vertical direction if Ag particles were interconnected and formed a sufficiently large mesh, no matter what the crystallographic orientation of Si substrate is.[22]

Conclusions

In summary, oxidation-rate-dependent etching of the (111) and (110) silicon substrates has been observed. In solutions with a high oxidant concentration, the etching prefers to proceed along the surface normal, whereas the etching tends to proceed along crystallographically preferred ⟨100⟩ directions in solutions with a low oxidant concentration. A similar change of the etching direction as a function of current density is observed during metal-assisted electrochemical etching. On the basis of these phenomena Si nanopores with modulated orientation directions can be fabricated. Furthermore, a tentative model has been developed to explain the etching behaviors by comparing the oxidation rate and dissolution rate of Si.

Acknowledgment. Thanks to Mr. H. Blumtritt for TEM samples preparation. Financial support from the German Research Foundation (STE 1127/8-1) is greatly acknowledged. We also acknowledge support by the European project NODE (IST 015783), the German-Israel DIP-project K6.1 managed by the German Research Foundation (DFG) (DFG project GO 704/5-1), and the research foundation of Jiangsu University, P.R. China (09JDG043).

Supporting Information Available: TEM image showing the orientation of a 50°-inclined etching, SEM images showing the morphology of *n*-type (111) Si substrates etched in solutions with different H_2O_2 concentrations, the morphology of *p*-type (111) Si substrate etched in solutions with different $Fe(NO_3)_3$ concentrations, and the morphology of *p*-type (111) Si substrate etched in solution with [HF]/[H_2O_2] = 230. This material is available free of charge via the Internet at http://pubs.acs.org.

References and Notes

(1) Schmidt, V.; Riel, H.; Senz, S.; Karg, S.; Riess, W.; Gösele, U. *Small* **2006**, *2*, 85.
(2) Goldberger, J.; Hochbaum, A. I.; Fan, R.; Yang, P. *Nano Lett.* **2006**, *6*, 973.
(3) Peng, K. Q.; Xu, Y.; Wu, Y.; Yan, Y. J.; Lee, S. T.; Zhu, J. *Small* **2005**, *1*, 1062.
(4) Garnett, E. C.; Yang, P. D. *J. Am. Chem. Soc.* **2008**, *130*, 9224.
(5) Fang, H.; Li, X. D.; Song, S.; Xu, Y.; Zhu, J. *Nanotechnology* **2008**, *19*, 255703.
(6) Chan, C. K.; Peng, H.; Liu, G.; McIlwrath, K.; Zhang, X. F.; Huggins, R. A.; Cui, Y. *Nature Nanotechnol.* **2008**, *3*, 31.
(7) Cui, Y.; Wei, Q.; Park, H.; Lieber, C. M. *Science* **2001**, *293*, 1289.
(8) Patolsky, F.; Zheng, G.; Lieber, C. M. *Nat. Protoc.* **2006**, *1*, 1711.
(9) Ma, D. D. D.; Lee, C. S.; Au, F. C. K.; Tong, S. Y.; Lee, S. T. *Science* **2003**, *299*, 1874.
(10) Hochbaum, A. I.; Chen, R. K.; Delgado, R. D.; Liang, W. J.; Garnett, E. C.; Najarian, M.; Majumdar, A.; Yang, P. D. *Nature* **2008**, *451*, 163.
(11) Buin, A. K.; Verma, A.; Svizhenko, A.; Anantram, M. P. *Nano Lett.* **2008**, *8*, 760.
(12) Hong, K. H.; Kim, J.; Lee, S. H.; Shin, J. K. *Nano Lett.* **2008**, *8*, 1335.
(13) Li, X.; Bohn, P. W. *Appl. Phys. Lett.* **2000**, *77*, 2572.
(14) Peng, K. Q.; Wu, Y.; Fang, H.; Zhong, X. Y.; Xu, Y.; Zhu, J. *Angew. Chem., Int. Ed.* **2005**, *44*, 2737.
(15) Tsujino, K.; Matsumura, M. *Adv. Mater.* **2005**, *17*, 1045.
(16) Huang, Z. P.; Wu, Y.; Fang, H.; Deng, N.; Ren, T. L.; Zhu, J. *Nanotechnology* **2006**, *17*, 1476.
(17) Huang, Z. P.; Fang, H.; Zhu, J. *Adv. Mater.* **2007**, *19*, 744.
(18) Huang, Z. P.; Zhang, X. X.; Reiche, M.; Liu, L. F.; Lee, W.; Shimizu, T.; Senz, S.; Gösele, U. *Nano Lett.* **2008**, *8*, 3046.

(19) Peng, K. Q.; Zhang, M. L.; Lu, A. J.; Wong, N. B.; Zhang, R. Q.; Lee, S. T. *Appl. Phys. Lett.* **2007**, *90*, 163123.

(20) Peng, K.; Lu, A.; Zhang, R.; Lee, S. T. *Adv. Funct. Mater.* **2008**, *18*, 3026.

(21) Chen, C. Y.; Wu, C. S.; Chou, C. J.; Yen, T. J. *Adv. Mater.* **2008**, *20*, 3811.

(22) Huang, Z. P.; Shimizu, T.; Senz, S.; Zhang, Z.; Zhang, X. X.; Lee, W.; Geyer, N.; Gösele, U. *Nano Lett.* **2009**, *9*, 2519.

(23) Geyer, N.; Huang, Z. P.; Fuhrmann, B.; Grimm, S.; Reiche, M.; Nguyen-Duc, T. K.; de Boor, J.; Leipner, H. S.; Werner, P.; Gösele, U. *Nano Lett.* **2009**, *9*, 3106.

(24) Choi, W. K.; Liew, T. H.; Dawood, M. K. *Nano Lett.* **2008**, *8*, 3799.

(25) Tsujino, K.; Matsumura, M. *Electrochem. Solid State Lett.* **2005**, *8*, C193.

(26) Zhang, X. G. *Electrochemistry of Silicon and Its Oxide*; Kluwer Academic/Plenum Publisher: New York, 2001.

(27) Zhang, M. L.; Peng, K. Q.; Fan, X.; Jie, J. S.; Zhang, R. Q.; Lee, S. T.; Wong, N. B. *J. Phys. Chem. C* **2008**, *112*, 4444.

(28) Tsujino, K.; Matsumura, M. *Electrochim. Acta* **2007**, *53*, 28.

(29) Lee, C. L.; Tsujino, K.; Kanda, Y.; Ikeda, S.; Matsumura, M. *J. Mater. Chem.* **2008**, *18*, 1015.

(30) Flatgen, G.; Wasle, S.; Lubke, M.; Eickes, C.; Radhakrishnan, G.; Doblhofer, K.; Ertl, G. *Electrochim. Acta* **1999**, *44*, 4499.

(31) Zeis, R.; Lei, T.; Sieradzki, K.; Snyder, J.; Erlebacher, J. *J. Catal.* **2008**, *253*, 132.

(32) Morinaga, H.; Suyama, M.; Ohmi, T. *J. Electrochem. Soc.* **1994**, *141*, 2834.

(33) Xia, X. H.; Ashruf, C. M. A.; French, P. J.; Rappich, J.; Kelly, J. J. *J. Phys. Chem. B* **2001**, *105*, 5722.

(34) Lehmann, V. *J. Electrochem. Soc.* **1993**, *140*, 2836.

(35) Lehmann, V.; Föll, H. *J. Electrochem. Soc.* **1990**, *137*, 653.

(36) Memming, R.; Schwandt, G. *Surf. Sci.* **1966**, *4*, 109.

(37) Peng, K. Q.; Fang, H.; Hu, J. J.; Wu, Y.; Zhu, J.; Yan, Y. J.; Lee, S. *Chem.—Eur. J.* **2006**, *12*, 7942.

(38) Chartier, C.; Bastide, S.; Levy-Clement, C. *Electrochim. Acta* **2008**, *53*, 5509.

(39) Xia, X. H.; Ashruf, C. M. A.; French, P. J.; Kelly, J. J. *Chem. Mater.* **2000**, *12*, 1671.

(40) Peng, K. Q.; Hu, J. J.; Yan, Y. J.; Wu, Y.; Fang, H.; Xu, Y.; Lee, S. T.; Zhu, J. *Adv. Funct. Mater.* **2006**, *16*, 387.

(41) Asoh, H.; Sakamoto, S.; Ono, S. *J. Colloid Interface Sci.* **2007**, *316*, 547.

(42) Ono, S.; Oide, A.; Asoh, H. *Electrochim. Acta* **2007**, *52*, 2898.

(43) Bressers, P. M. M. C.; Kelly, J. J.; Gardeniers, J. G. E.; Elwenspoek, M. *J. Electrochem. Soc.* **1996**, *143*, 1744.

(44) Lee, J.; Farhangfar, S.; Lee, J.; Cagnon, L.; Scholz, R.; Gösele, U.; Nielsch, K. *Nanotechnology* **2008**, *19*, 365701.

JP911121Q